

Formulation of Phytosomes Containing *Rubia cordifolia* Extract for Neuropathic Pain: *In Vitro* and *In Vivo* Evaluation

Nitin Kumar,* Radha Goel, Mohd Nazam Ansari, Abdulaziz S Saeedan, Hasan Ali, Neeraj Kant Sharma, Vaishali M. Patil, Dinesh Puri, and Monika Singh



Cite This: *ACS Omega* 2024, 9, 25381–25389



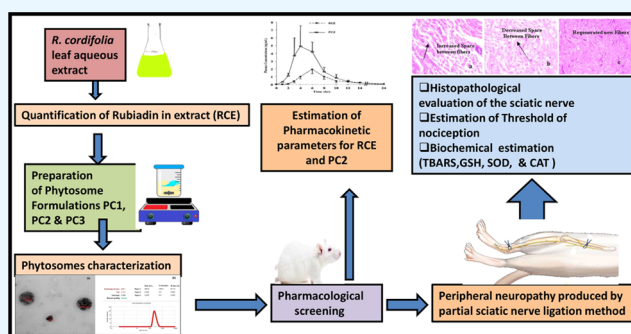
Read Online

ACCESS |

Metrics & More

Article Recommendations

ABSTRACT: This study aimed to develop a delivery system for the dried aqueous extract of *Rubia cordifolia* leaves (RCE) that could improve the neuroprotective potential of RCE by improving the bioavailability of the chief chemical constituent rubiadin. Rubiadin, an anthraquinone chemically, is a biomarker phytoconstituent of RCE. Rubiadin is reported to have strong antioxidant and neuroprotective activity but demonstrates poor bioavailability. In order to resolve the problem related to bioavailability, RCE and phospholipids were reacted in disparate ratios of 1:1, 1:2, and 1:3 to prepare phytosome formulations PC1, PC2, and PC3, respectively. The formulation PC2 showed particle size of 289.1 ± 0.21 nm, ζ potential of -6.92 ± 0.10 mV, entrapment efficiency of 72.12%, and *in vitro* release of rubiadin of 89.42% at pH 7.4 for a period up to 48 h. The oral bioavailability and neuroprotective potential of PC2 and RCE were assessed to evaluate the benefit of PC2 formulation over the crude extract RCE. Formulation PC2 showed a relative bioavailability of 134.14% with a higher neuroprotective potential and significantly ($p < 0.05$) augmented the nociceptive threshold against neuropathic pain induced by partial sciatic nerve ligation method. Antioxidant enzyme levels and histopathological studies of the sciatic nerves in various treatment groups significantly divulged that PC2 has enough potential to reverse the damaged nerves into a normal state. Finally, it was concluded that encapsulated RCE as a phytosome is a potential carrier system for enhancing the delivery of RCE for the efficient treatment of neuropathic pain.



1. INTRODUCTION

Out of all the pain and suffering, neuropathic pain (NP), which is caused by injury or damage to the nerves, and manifests as tingling, shooting, burning, stabbing pain, or shocking, is the most horrifying. Diabetes is the most common cause of neuropathy. It may also be caused by other health conditions like cancer, hypertension, anxiety, poor nutrition, and intake of some anticancer and antimycobacterial drugs, for example, Paclitaxel, Vincristine, Dapsone, Isoniazid, Rifampin, etc. To treat NP, a wide range of drugs are available, including opioids, NSAIDs, antidepressants, and anticonvulsants. Serious side effects are present in the majority of these adverse effects despite the need for safe treatment. The use of antidepressants and NSAIDs increases the risk of gastrointestinal adverse effects like peptic ulcer, acidity, and diarrhea. Herbs are a natural source of many bioactive compounds, including specific glycosides and polyphenols, which act as potent antioxidants *in vivo* to mediate the suggested health benefits.^{1,2} Therefore, in terms of the possibility of a successful therapeutic outcome, herbal treatment might offer a better alternative.

A member of the Rubiaceae family *Rubia cordifolia* includes the chemical compound *rubiadin*, a derivative of hydroxy

anthraquinone. For a very long time, *R. cordifolia* has been used as an antibacterial and to treat rheumatoid arthritis, uterine pain, and joint pain.³ Furthermore, *R. cordifolia* has been linked to hepatoprotective, nephroprotective, antineoplastic, anti-ulcer, anti-inflammatory, and antidysenteric properties.⁴ *R. cordifolia* root extract demonstrated antioxidant and antihyperglycemic effects in a previous study.^{5,6} In a different study, the aqueous root extract of *R. cordifolia* was tested for its antidiabetic properties using a diabetic rat model that was induced using streptozocin.⁷ Additionally, the alcohol extract from *R. cordifolia* demonstrated antioxidant and antihyperglycemic properties in a different study.⁸ According to other studies, *R. cordifolia* root extract has shown strong antioxidant and antidiabetic properties. Poor stability and absorption have been observed in a number of herbal compounds, including

Received: April 19, 2024

Revised: May 13, 2024

Accepted: May 16, 2024

Published: May 27, 2024



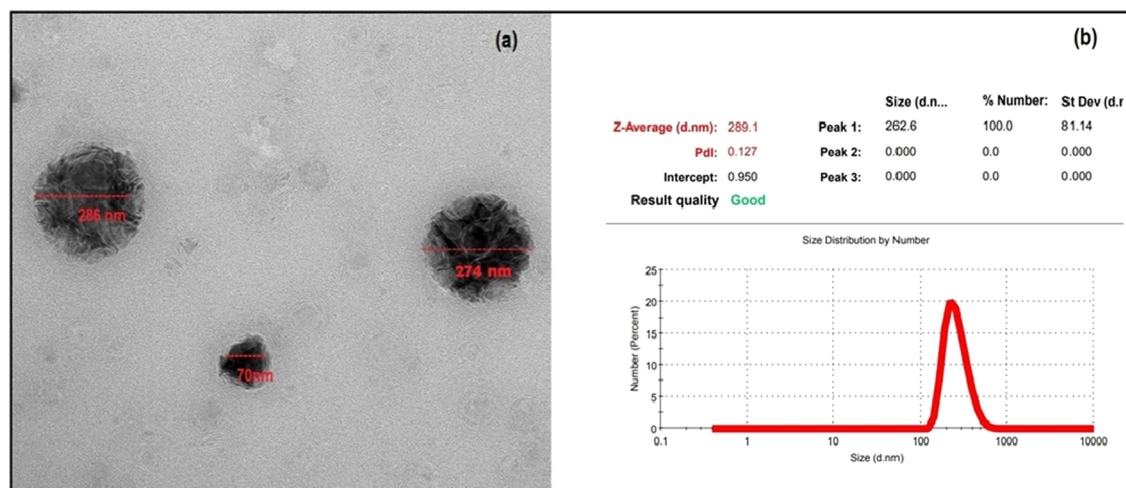


Figure 1. Photographs of PC2 formulations showing the (a) morphology of the phytosome vesicles by TEM, and (b) particle size distribution of PC2 formulation.

Table 1. Mean Diameter (Dmean) of Particle Size, Polydisparsity Index (PDI), ζ Potential, and % Entrapment Efficiency of Phytosome Formulations^a

formulation	size Dmean (nm)	PDI	ζ potential	% entrapment efficiency
PC1	805.2 \pm 1.4	0.285 \pm 0.03	-5.85 \pm 0.14	48.78 \pm 0.52
PC2	289.1 \pm 0.21	0.127 \pm 0.01	-6.92 \pm 0.10	84.32 \pm 0.22
PC3	721.5 \pm 0.28	0.207 \pm 0.02	-7.12 \pm 0.23	44.61 \pm 0.40

^aAll of the values are presented as the mean \pm standard deviation ($n = 3$).

rubiadin. These traits modify the way in which rubiadin is absorbed, potentially impacting the compound's ability to treat various medical conditions.⁹ There have been several reports of attempts to increase the solubility of poorly soluble drugs, which has improved gastrointestinal permeability and, consequently, drug bioavailability. Certain substances have cytotoxic, neuroprotective, and anti-inflammatory properties.¹⁰ In the clinic, the entire plant is used to treat a variety of tumors, intestinal abscesses, boils and scalded tissues, and malaria. Rubiadin is the main constituent of *R. cordifolia* leaves.¹¹ It makes up about one-sixth of all bioactive substances. Rubiadin was previously found to have strong antioxidant properties. However, because of its poor solubility and less permeability in the intestinal lumen, it has a much lower absorption following oral administration. Different phytoconstituents such as anthraquinone, flavonoids, and saponins form reversible complexes with phospholipids and showed long-lasting therapeutic effects than those observed after administration of the same amount of substance in free form due to poor bioavailability.¹² By utilizing a phytosome delivery system, which increases the rate, as well as the extent of the compounds into the intestinal fluids and permits cross-biomembrane transport, the low oral bioavailability of the herbal extracts can be improved. Previously, in a study, it was also proved that wound healing potential of *Piper cubeba* oil may be enhanced via self-nanoemulsifying nano lipid drug delivery system in comparison with standard gentamycin.¹³ Phytosomes, a commercial form of many popular standardized herbal extracts, including *Ginkgo biloba*, *Silybum marianum*, *Vitis vinifera*, *Glycyrrhiza glabra*, *Panax ginseng*, *Curcuma longa*, and *Centella asiatica*, is currently available.^{14,15} A review of the literature also showed that pomegranate extract-loaded phytosomes increased punicalagin's serum bioavailability more than extracts by themselves.¹⁶ In another study, it is

again reflected that use of nanoparticles as a novel formulation of ZnO-Manjistha extract enhanced antimicrobial and antioxidant activity.¹⁷ In a different investigation, the outcomes of phytosomes made with mixtures of alcoholic extracts from *Abutilon indicum* leaves and *Piper longum* fruits were contrasted with those of alcoholic extracts from each plant alone. Liver damage markers are reduced by phytosomes more than by extracts alone.¹⁸

Plant extracts and phospholipids are combined in phytosomes, which are nanoformulations, to create fat-soluble complexes.¹⁹ The extract establishes a covalent connection with the phospholipids without being encapsulated as these complexes' core.²⁰ Because of the fat-soluble, biocompatible extract phospholipid complex, phytosomes maximize the active element's bioavailability while also protecting it.^{21,22} Thus, the preparation and analysis of phytosomes loaded with RCE (*R. cordifolia* leaf extract) were the goals of this study. The improved formulation's numerous distinguishing features and neuroprotective qualities in animal design have been examined. An oral bioavailability study was conducted for the improved formulation in order to ascertain the bioavailability and a number of pharmacokinetic parameters.²³

2. RESULTS AND DISCUSSION

2.1. Characterization of RCE. RCE has been a darker green powder with a disagreeable taste and alkalinity (pH 8), with a 185 °C melting point.

2.2. Quantification of Rubiadin in RCE. A standard curve has been formed to quantify the rubiadin in RCE. Rubiadin was found to be 3.05% w/w in RCE.

2.3. Characterization of Phytosomes. **2.3.1. Morphological Study.** Most of the phytosomes are composed of amphiphilic molecules called phospholipids, which have two neutral tail groups and one positive headgroup. Moreover,

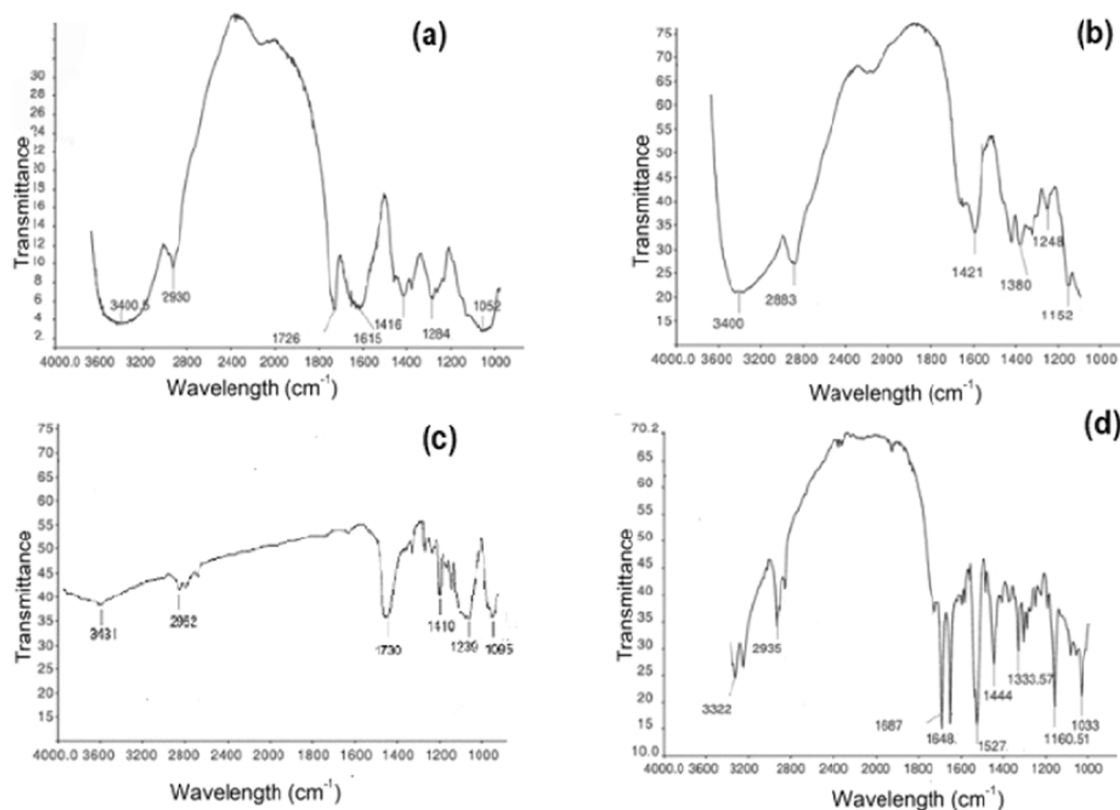


Figure 2. FTIR spectra: (a) phospholipids, (b) phospholipids and RCE mixture, (c) RCE, and (D) PC2.

when rubiadin was mixed with phospholipids to form a complex component, it became more soluble. On the basis of these outcomes obtained via TEM, phytosome formulation PC2 was found to be more spherical than phytosome formulations PC1 and PC3 (Figure 1).

2.3.2. ζ Potential, PDI, and Particle Size Distribution. Table 1 contains a list of the particle size distributions. Formulations PC1, PC2, and PC3 showed mean diameter of particle 805.2 ± 1.4 , 289.1 ± 0.21 , and 721.5 ± 0.28 nm, respectively. The PDI indicates a particle's homogeneity in the dispersion. With the PC2 formulation, the particle size homogeneity was best indicated by the lowest PDI value of 0.127 (Figure 1). ζ potential was evaluated for its stability (range: +30 to -30 mV), and the values of the various formulations PC1, PC2, and PC3 were -5.85 ± 0.14 mV, -6.92 ± 0.10 mV, and -7.12 ± 0.23 mV, respectively.

2.3.3. Entrapment Efficiency. PC2 formulation entrapped 84.32% rubiadin, whereas PC1 and PC3 formulations entrapped 48.78 and 44.61%, respectively (Table 1). Hence, PC2 has been chosen for further analysis due to its highest entrapment efficiency.

2.3.4. FTIR Interpretation. In comparison to those of the -OH group in RCE, phospholipids, and their physical combination, the -OH peak intensity of the PC2 formulation has been lower. Because of the hydrogen bonding among the RCE and the phospholipids complex, OH peaks were observed at 3400 cm^{-1} , but in the phospholipids, RCE, and PC2, -OH peaks were observed at 3400.5 cm^{-1} , 3431 cm^{-1} , and 3322 cm^{-1} , respectively. But when the two compounds were physically combined, the peak intensity of -OH did not decrease, suggesting that there were no H-bond among them (Figure 2).

2.3.5. DSC Analysis. RCE was detected in the phytosomes by a DSC analysis. At $138.61\text{ }^\circ\text{C}$, a broad endothermic peak corresponding to phospholipids was visible on the DSC thermogram. At $145\text{ }^\circ\text{C}$, the pointed ENP of the RCE was detected. There were two peaks on the PC2 thermograph, at 82.41 and $108.20\text{ }^\circ\text{C}$. The peak intensities showed a slight decrease when compared to the original sample. The phospholipids' and RCE's organic hydrophobic interactions could be the cause of this difference. In contrast, PC2's notable peak at $108.20\text{ }^\circ\text{C}$ entirely disappeared, leaving only the material's melting point at $126.41\text{ }^\circ\text{C}$ (Figure 3). This might be the result of RCE and phospholipids forming a complete and firmly bound complex, which stopped the extract from dissociating into PC2 at the time of processing.

2.3.6. In Vitro Release. The PC2 formulation depicted minimum drug release in the simulated fluid of the stomach (pH 1.2). At pH 7.4, PC2 exhibited a more controlled release of the active ingredient rubiadin as compared to other formulations. Moreover, PC2 depicted about 89.42% of the total cumulative release for 48 h (Figure 4).

2.4. Pharmacological Screening. **2.4.1. Acute Toxicity Studies.** No toxic effects were seen in adult male albino rats after 20 days of administration of 500 mg/kg/day of RCE (equivalent to 15.25 mg of rubiadin) and 4000 mg/kg/day of RCE (equivalent to 122 mg of rubiadin) intraperitoneally and orally, respectively.

2.4.2. Evaluation of Neuroprotective Potential. **2.4.2.1. In Vivo Biochemical Estimation via Sciatic Nerve Tissue.** Antioxidant enzyme levels (SOD, catalase, and reduced glutathione) significantly increased in the rats treated with PC2, while MDA/TBARS levels significantly decreased. The TBARS level was significantly lower in those treated with PC2

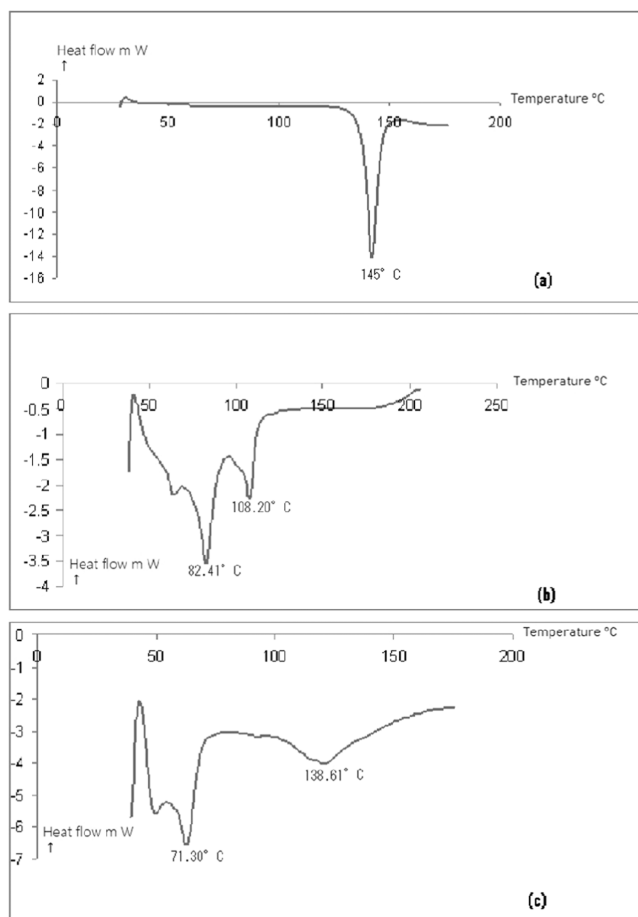


Figure 3. DSC thermogram images showing (a) RCE, (b) PC2, and (c) phospholipids.

compared to those in groups I, II, and III ($p < 0.01$). A comparison of the RCE-treated group II to the PC2-treated group III and the negative control group I revealed that the RCE treatment considerably ($p < 0.01$) decreased the amount of total bilirubin (TBARS). Comparing the negative control group, the amount of TBARS was considerably lower in the RCE treatment group ($p < 0.01$) (Figure 5). GSH, SOD, and catalase levels significantly increased in rats given PC2. These findings led to the conclusion that the PC2 formulation was the most effective means of significantly lowering the level of oxidative stress. Oxidative stress is the primary cause of neuropathic pain and a number of other neurological disorders.²⁴

2.4.2.2. Effect on Paw Withdrawal Latency/Threshold of Nociception. On day seven of the therapy, compared with those of the negative control rats, the mechanical allodynia of the treated groups II & III was substantial. Its effectiveness in treating neuropathic conditions was demonstrated by the increased mechanical allodynia in the treated groups. Compared to those in groups I & II on days 7 as well as 14, the paw withdrawal latency in PC2-treated rats (group III) substantially increased (Table 2). Compared to those in the negative control group (group I), the paw withdrawal latency of the rats in the RCE-treated group (group II) substantially increased on the 7th and 14th days. As a result, following sciatic nerve ligation, rats were given PC2, or 40 mg/kg/day rubiadin, which showed the greatest effect on reducing the nociceptive threshold. The neuroprotective impact seen in the

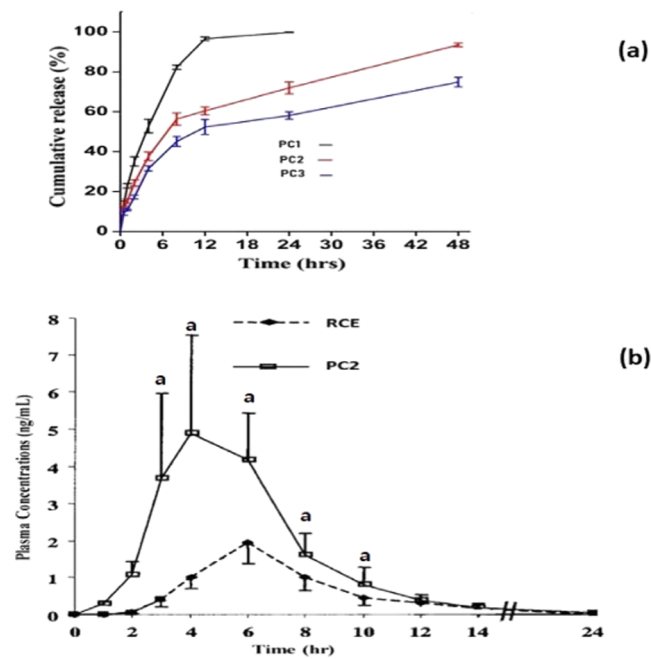


Figure 4. (a) *In vitro* cumulative release patterns of rubiadin at pH 7.4 obtained from *in vitro* dissolution tests of the formulations (PC1, PC2, and PC3) consisting of RCE and phospholipids in varying ratios of 1:1, 1:2, and 1:3, respectively. The estimated values were given as mean \pm SD; $n = 3$. (b) Graph displaying mean plasma concentration versus time profile following oral administration of PC2 and RCE at a dosage of 40 mg/kg rubiadin. The values were estimated using mean \pm SEM for $n = 6$, with “a” denoting statistical significance at $p < 0.05$ based on RCE. Animals in Group II were given a single oral dosage of RCE, which is equal to 40 mg/kg/day of rubiadin, and Group III was given a single oral dose of PC2, which is equal to 40 mg/kg/day of rubiadin. Blood samples were taken from animals.

rats given PC2 treatment suggests that the best way to increase the threshold against pain transmission may be to administer RCE via PC2 formulation.

2.4.2.3. Histopathological Evaluation of the Sciatic Nerve. From the histopathology images in group I, it was obvious that some unmyelinated and myelinated fibers had deteriorated and others had swollen. There were fewer gaps among the fibers in groups II & III, as demonstrated by the sciatic nerve histology in the treated groups. However, comparing it with those in groups I & II, the differences in edema in group III were very insignificant (Figure 6). The present study showed that PC2 has a higher neuroprotective effect as compared to RCE or the negative control group and might be utilized to treat NP.

2.4.3. Oral Bioavailability Studies. The results of the pharmacokinetic investigation included information on the slow elimination phase and the evident absorption phase (Figure 4). The T_{max} values for RCE and PC2 were 6.2 and 4.1 h, respectively, and were significantly different from one another. Similarly, significant changes in T_{1/2} for both RCE and PC2 were also observed. Nevertheless, after the same dose was taken orally (equivalent to 40 mg/kg rubiadin) in both treatment groups, various peak concentrations (C_{max}) were attained. After 4 h of PC2 administration, the C_{max} was 4.89 μ g/mL, which was estimated to be 2.25-fold greater than that of RCE, as shown in Table 3. In contrast to the other treatments, PC2 had higher levels of the drug in the blood at every time point. The AUC of PC2 and RCE has been found to be 28.13 \pm 2.81 and 19.21 \pm 1.21, respectively. Hence, PC2

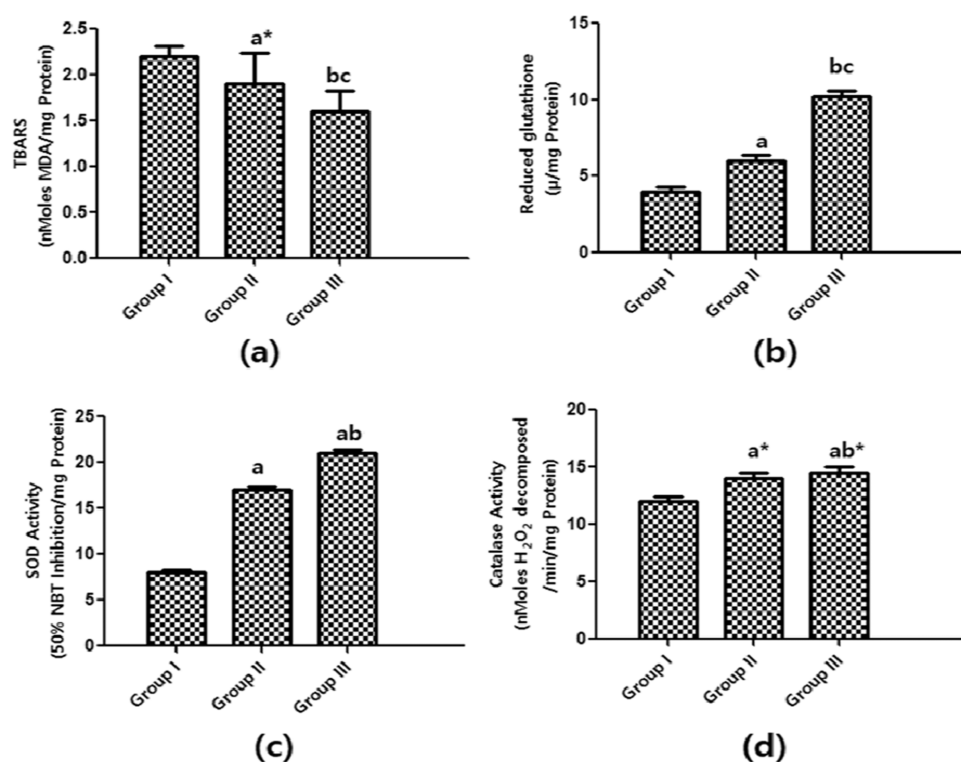


Figure 5. Images of bar graphs exhibiting (a) TBARS, (b) GSH, (c) SOD, and (d) CAT levels in treatment groups I, II, and III. The values are presented as mean \pm SEM ($n = 6$); ^a = $p < 0.05$ when analogized with Group I; ^{a*} = $p < 0.05$ not significant when compared with Group I; ^b = $p < 0.05$ significant when analogized to Group II; ^{b*} = $p < 0.05$ not significant when analogized to Group II; ^c = $p < 0.05$ significant when analogized to Group III (ANOVA^a followed by Dennett's test).

Table 2. Effect on Threshold of Nociception in Rats Measured by Paw Withdrawal Latency, Observed before and after the Treatments

treatment groups	paw withdrawal latency (s)		
	0th day	7th day	14th day
Group I (negative control group)	4.13 \pm 0.25	3.4 \pm 0.14	3.18 \pm 0.03
Group II (RCE-treated group)	2.35 \pm 0.20	1.91 \pm 0.05 ^a	1.35 \pm 0.54 ^a
Group III (PC2-treated group)	0.85 \pm 0.02	0.46 \pm 0.01 ^{a,b}	0.31 \pm 0.01 ^{a,b}

^aThe values were estimated in mean \pm SEM ($n = 6$); ANOVA followed by Dunnett's test; 'a' indicates statistical. ^bSignificance for Group I; 'b' indicates significance for Group II at $p < 0.05$.

showed a relative bioavailability of 134.14% as compared to RCE for a period of 24 h. The findings indicated that phospholipids may increase PC2's oral bioavailability, but the

Table 3. Observations on Pharmacokinetic Parameters for RCE and PC2 after Oral Administration^a

pharmacokinetic parameters	treatments	
	RCE	PC2
Cmax ($\mu\text{g/mL}$)	1.98 \pm 0.01	4.89 \pm 0.11
Tmax (h)	6.2 \pm 0.11	4.1 \pm 0.16
T1/2 (h)	7.27 \pm 1.37	7.98 \pm 0.33
AUC _{0-t} ($\mu\text{g h/mL}$)	19.21 \pm 1.21	28.13 \pm 2.81
Mean residence time (h)	15.13 \pm 1.35	8.14 \pm 0.38
Relative bioavailability (%)	100	134.14

^aAll values are presented as mean \pm SEM ($n = 6$).

PC2 delivery mechanism may increase those drug carriers' effectiveness considerably more.

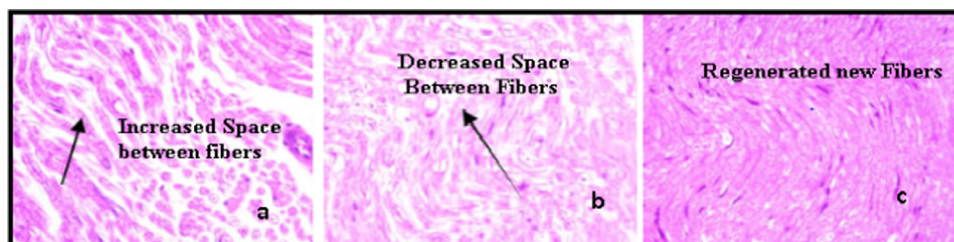


Figure 6. Photographs of sciatic nerves histopathology (images at $\times 200$ stained with eosin and hematoxylin) on PSNL-induced neuropathic pain in different treatment groups: (a) Group I, negative control; (b) Group II, single dosage of RCE orally equivalent to 40 mg/kg/day of rubiadin; and (c) Group III: Single dosage of PC2 orally equivalent to 40 mg/kg/day of Rubiadin.

3. CONCLUSIONS

The results demonstrated that, after up to 24 h, the RCE delivery via the phytosome formulation improved the bioavailability and also enabled the more controlled release of rubiadin in an alkaline dissolution medium. RCE's antioxidant capacity was enhanced by the PC2 formulation, which had a neuroprotective effect. Unlike earlier treatments, sciatic nerve histopathological analysis confirmed that the RCE distribution via the PC2 formulation was effective in regenerating nerve fibers. PC2 showed greater C_{max} , T_{max} , and AUC values than did the other treatments in this study, which enhanced the oral bioavailability of the phytoconstituent rubiadin. Although the PC2 delivery system is likely to improve the effectiveness of these carriers of drug and achieve notable rises in oral bioavailability and pharmacological effectiveness, this research has confirmed that phospholipids can raise the phytoconstituents' bioavailability.

4. METHODS

4.1. Materials. *R. cordifolia* leaf aqueous extract was obtained from Sistropic Naturemed Pvt. Limited, India. Biomarker Rubiadin and Phospholipids, which are marketed as *L*- α -phosphatidylcholine, have been procured from Sigma-Aldrich. For the purpose of testing biochemical parameters, kits of standards from Erba Diagnostics in New Delhi, India, were needed. All of the chemical solvents as well as reagents used for the entire experiment were of analytical grade.

4.2. Characterizations of *R. cordifolia* Extract (RCE).

4.2.1. Physical Characteristics. Organoleptic evaluation, which considers appearance, color, odor, and taste, was used to identify the RCE. By dipping the electrodes of a pH meter (Manti Lab MT) into a 5 mL solution of RCE, which was made by diluting 1 g of RCE with 10 mL of the purified water, at 25 °C, the pH was ascertained. Differential scanning calorimetry (PerkinElmer DSC 8500/8500) was used to find the melting point.

4.2.2. Rubiadin Assay in *R. cordifolia* Extract. The calibration curve for the quantification of rubiadin in RCE was prepared using a standard solution (10–60 $\mu\text{g}/\text{mL}$) of rubiadin from Alfa Biotech Limited. HPLC (Shimadzu LC-10AD) was utilized, running on a C18 column and using a UV detector at 203 nm, to ascertain the percentage content of rubiadin in the RCE. In this evaluation, acetic acid (0.05% v/v):acetonitrile (85:15, v/v) was utilized as the mobile phase.

4.3. Preparation of Phytosomes Formulation. Phospholipids and RCE were combined in w/w ratios of 1:1, 1:2, and 1:3 to form entrapment efficiency of formulations of phytosome termed as PC1, PC2, and PC3, respectively, based on the percentage content of the bioactive compound rubiadin (molecular weight, 1221.38 g/mol) in RCE. Additionally, 200 mg of RCE was combined with 60 mL of 90% ethanol in a beaker along with 400 mg of phospholipid and 60 mL of dichloromethane. The 2 beaker contents (solutions) have been combined in a flask with a flat bottom using the w/w ratios for PC1, PC2, and PC3 as previously mentioned. The solvents were removed until a thin film layer was created by operating a Buchi rotary vacuum evaporator at the rotational speed of 2 rpm and the temperature of 37 °C. The mixture was then hydrated, and the phytosomes were suspended by the addition of distilled water. The R230 Focused ultrasonicator was used to resuspend the phytosomes for careful optimization of their size as well as shape.²⁵ The phytosomes were first dried by

freeze-drying (Lyophilizer-Labconco, Model 7934000) for 1 day at -40 °C and 40 mbar of pressure, then by secondary drying for an additional day at 25 °C. This process was done prior to phytosome characterization. Following the samples' removal from the dryer, the product was kept at 4 °C in a desiccator above phosphorus pentoxide (P_2O_5) until further analysis.

4.4. Phytosome Characterization. **4.4.1. Morphological Study.** Phytosome morphology was calculated via transmission electron microscopy (TEM), Philips CM 10, Holland.

4.4.2. ζ Potential, Polydispersity Index, and Particle Size Distribution Study. The polydispersity index (PDI), ζ potential (ZP), and particle size (PS) distribution of the phytosomes were calculated via DLS (dynamic light scattering) and a PS analyzer by utilizing a computerized system (PCS; Zetasizer Malvern, UK).

4.4.3. Estimation of Entrapment Efficiency. Centrifuging was used to estimate the entrapment efficiency. Each formulation (PC1, PC2, and PC3) was centrifuged in a 0.5 mL suspension at 10 000 rpm for 15 min at room temperature using a Remi PR-24 Research Centrifuge. For vesicle disruption, the supernatants from formulations PC1, PC2, and PC3 were combined with ethanol in volumes of 0.20, 0.30, and 0.25 mL, respectively. For the estimation of entrapment efficiency, supernatants were obtained from each formulation in the relevant dissolution medium. The concentration of rubiadin in the supernatant (encapsulated rubiadin) of PC1, PC2, and PC3 was estimated by utilizing spectrophotometry (Shimadzu 1800, Japan) at 203 nm. The percent entrapment efficiencies of PC1, PC2, and PC3 have been computed in regard to the rubiadin encapsulated in each and every formulation.²⁶

4.4.4. In Vitro Drug Release Studies. For PC2, a USP Type-II dissolution test apparatus (Labindia DS 8000, India) was used to perform *in vitro* drug release. Buffer having pH 1.2 for 2 h and pH 7.4 after 2 h were the media used for the release study; these were used to simulate intestinal and gastric fluids, respectively. A 500 mL paddle of a dissolution test apparatus containing sufficient dissolution medium was used to tie the phytosomes to the membrane after they had been precisely weighed at 50 mg and placed in a cellulose dialysis membrane with the molecular weight removed at 14 KD. Dissolution was carried out at 37 ± 0.5 °C and 100 rpm. The same volume of freshly warmed solution was mixed after each withdrawal to maintain the medium concentration. Aliquots (5 mL) were taken using a pipette at prearranged intervals. The obtained samples were subjected to HPLC analysis in order to ascertain the rubiadin content.²⁷

4.4.5. Fourier Transform Infrared (FTIR) Spectroscopic Study. Using KBr disks, infrared spectroscopy (FT/IR-4000) based in Jasco, Japan, was utilized to investigate the relationship between phospholipids and RCE. Calculations have been conducted in the scanning range of $4000\text{--}400\text{ cm}^{-1}$ for RCE, PC2, and phospholipids.

4.4.6. DSC Analysis. Moreover, PC2 and phospholipid thermograms were calculated using DSC (PerkinElmer 8500/8500).

4.5. Pharmacological Screening. **4.5.1. Animals.** All pharmacological studies were conducted on adult male albino rats weighing 150–160 g. Water and food were provided in the cages housing the rats.

4.5.2. Ethical Approval. The Lloyd Institute of Management and Technology's Institutional Animal Ethical Commit-

tee (IAEC) gave its approval, and the study was carried out as per CPCSEA India guidelines.

(IAEC Application Approval Number 1206/PO/Re/S/O8/CPCSEA/09/2022)

4.5.3. Acute Toxicity Studies. The previously published methodology was followed in performing the single-dose safety evaluation of RCE.^{28,29} One group of rats receiving 500 mg/kg RCE (equivalent to 15.25 mg of rubiadin) intraperitoneally once daily, and another group of rats were given an oral single dose of 4000 mg/kg (equal to 122 mg of rubiadin) for 20 days, in both groups. At the conclusion of the experiment, hematological parameters were reported to be normal. During the experiment, other laboratory parameters such as the consumption of food, body weight, ophthalmologic investigations, urine investigations, and behavior were also assessed, and the findings were observed to be normal.

4.5.4. Experimental Protocol for Evaluation of Neuroprotective Potential. The rats were given intraperitoneal injections of xylazine (5 mg/kg) and ketamine (50 mg/kg) to induce anesthesia. After disinfection with iodine, the right thigh has been shaved. The sciatic nerve was visible after the right upper thigh had been dissected. The sciatic nerve was securely removed, and the dorsal half was attached using an 8–0 silk suture. Two muscle sutures and 3–4 skin sutures have been utilized to close the incisions after the procedure. The rats were given 2 days to recover following surgery. We saw behavioral indicators of hyperalgesia and pain.³⁰

Three categories were created at random from these rats, with six “rats in each:

Group I: Given 2 mL/kg daily dosage of saline orally, negative control group

Group II: Single dose of RCE orally (same as 40 mg/kg/day of Rubiadin)

Group III: Single dose of PC2 orally (same as 40 mg/kg/day of Rubiadin)

4.6. In Vivo Biochemical Estimation via Sciatic Nerve Tissue. *In vivo* measurements of antioxidant marker enzymes were carried out at the end of the research (i.e., on the 14th day). To collect nerve tissue for biochemical analysis, the rats were sacrificed by cervical dislocation. The muscles were separated, and the sciatic nerve was isolated using scissors and forceps without causing damage to blood vessels. Each rat's sciatic nerves, which measure about 1.5 cm each, were collected and placed in an Eppendorf tube filled with 0.1 M PBS.³¹

4.6.1. Tissue Preparation. Preparation of 10%w/v tissue homogenates was performed in 0.1 M PBS (pH 7.4) at 15000 rpm for 20 min, followed by biochemical estimation. The samples were then centrifuged at 20,000 rpm for 60 min at a temperature of 4 °C to extract the other enzymes, and the postnuclear supernatant fraction was exposed to catalase activity at the rotational speed of 5000 rpm for 20 min at 4 °C.

4.6.2. Lipid Peroxidation Assay. The assay was carried out using earlier procedures. Using a spectrophotometry set at 535 nm, the amount of malondialdehyde (MDA) was estimated. The outcomes are shown as nanomolars generated per mg of tissue protein. Thiobarbituric acid reactive (TBAR) was calculated using the formula nM MDA/mg protein.³² The protein content was ascertained by a previously reported method³³ utilizing bovine serum albumin as a reference.

4.6.3. Reduced Glutathione (GSH) Estimation. This parameter has been determined using a previously published technique.³¹ Sulfosalicylic acid (4%w/v, 1 mL) was used to

precipitate one milliliter of supernatant through a cold digestion procedure at a temperature of 4 °C for about 1 h. Following that, the sample was centrifuged for 15 min at 6000 rpm and 4 °C. Following centrifugation, 1 mL of the supernatant was removed, and 0.2 mL of 5,5-dithiobis (2-nitrobenzoic acid) (DTNB) and 2.7 mL of PS (0.1 M, pH 8) were added. A yellow color developed as a result of this. At 412 nm, the developed color's intensity was measured spectrophotometrically. Micromoles (μM) per gram of tissue weight are the expression for the chromophore's molar extinction coefficient, which was calculated to be $1.36 \times 10^4 \text{ M}^{-1} \text{ cm}^{-1}$.³⁴

4.6.4. Superoxide Dismutase. The pyrogallol autoxidation hindrance has been used to measure the activity of superoxide dismutase (SOD).³⁵ The absorbance has been observed at 420 nm following the addition of 100 μL of cytosolic supernatant and 25 μL of pyrogallol to Tris HCL buffer.

4.6.5. Catalase. To extract the supernatant, the tissue homogenate was centrifuged with 2 mL of PBS at 3000 rpm for about 15 min. To 50 μL of cytosolic supernatant, 2.95 mL of 19 nM H_2O_2 was added at 1 min intervals for 3 min. Catalase is needed to break down H_2O_2 . After the reaction, 2 mL of this solution was added to quartz cuvettes at various times, and the absorbance was measured by using spectrophotometry to determine the amount of H_2O_2 that had degraded. First, the H_2O_2 first-order reaction was followed by H_2O_2 decomposition. Catalase activity was measured in nanomolars (nM) for each milligram of protein and each minute that hydrogen peroxide was encapsulated.^{36,37}

4.7. Nociceptive Threshold Evaluation. The dynamic mechanical allodynia paint brush behavior framework was utilized to calculate the nociceptive threshold. The animals were put in a cylinder with a wired mesh floor, and the plantar surface of each animal's paw was stroked with a paint brush to produce a stimulus. The total withdrawals were counted five times after the stimulation, separated by five seconds each time.³⁸

4.8. Histopathological Examination. Sliced to a thickness of 4 mm, sciatic nerve samples were preserved in a 10% formalin fixative solution and stained with eosin along with hematoxylin. A light microscope (400 \times) was used to look for histopathological degenerative alterations in the sections.

4.9. Oral Bioavailability Studies. Before beginning the experiment, six male adult rats weighing between 150 and 160 g were split into two groups and given a 12 h fast. Two groups were given different doses of rubiadin: 40 mg/kg PC2 and RCE, respectively. At different intervals of 1, 2, 4, 8, 16, and 24 h, samples of blood from the retro-orbital plexus have been obtained and stored in 1.5 mL micro centrifuge tubes. Following a 10 min centrifugation at 3000g, the plasma was extracted from the blood and kept cold until further analysis. 100 μL of plasma and 1.0 mL of 2.0 M HCL were placed in each test tube. The mixture was heated to a temperature of 80 °C for 1.5 h and then allowed to cool to room temperature in order to hydrolyze it. In this reaction medium, 1.0 mL of ethyl acetate was combined. Following a 3 min vortex, this mixture was centrifuged for 10 min. After the process of centrifugation, the supernatant was collected and vacuum desiccators were used to dry it. Following drying, the material was reconstituted in 100 μL of the mobile phase and analyzed quantitatively using LC-MS/MS (Model: TSQ Quantum, Thermo Fisher Scientific, Inc., USA).³⁹ A triple quadrupole mass spectrometer was employed in this study. The stationary phase of a C18-HPLC column with 5 m-PS was kept at 25 °C. The mobile

phase consisted of 0.1% v/v formic acid and methanol at a flow rate of 1.5 mL/min. Rubiadin was used to standardize this process in order to achieve the greatest peak resolution feasible. At 203 nm, chromatographic peaks are easily observed in the quantitative analysis. Selected reaction monitoring was used in a positive ionization mass spectrometric analysis of the material. The target ions for rubiadin have been found at 1109.61m/z.⁴⁰ LCQUAN Software (Thermo Fisher Scientific, Inc., USA) was used to carry out peak integration analysis and data collection. Disparate pharmacokinetic parameters: (a) half-life ($t_{1/2}$), (b) maximum plasma concentration (C_{max}), and (c) relative bioavailability were estimated via statistical software. (d) Mean residence time (MRT), (d) area under the curve: plasma concentration v/s time (AUC_{0-t}), and (f) time to reach C_{max} (T_{max}).

5. STATISTICAL DATA ANALYSIS

In vitro results are represented as mean ± SD (standard deviation). The antioxidant potential and *in vivo* pharmacokinetics were calculated using mean ± SEM (standard error of the mean). *P* values of less than 0.05 denote statistical significance. Dennett's test as well as one-way ANOVA was utilized for the statistical analysis.

AUTHOR INFORMATION

Corresponding Author

Nitin Kumar – Department of Pharmacy, Meerut Institute of Technology, Meerut 250103, India; orcid.org/0000-0003-4473-6418; Phone: +919897693004; Email: nitin@mitmeerut.ac.in

Authors

Radha Goel – Department of Pharmacology, Lloyd Institute of Management and Technology, Greater Noida 201306, India

Mohd Nazam Ansari – Department of Pharmacology and Toxicology, College of Pharmacy, Prince Sattam Bin Abdulaziz University, Alkharj 11942, Saudi Arabia; orcid.org/0000-0001-8580-3002

Abdulaziz S Saeedan – Department of Pharmacology and Toxicology, College of Pharmacy, Prince Sattam Bin Abdulaziz University, Alkharj 11942, Saudi Arabia

Hasan Ali – Department of Pharmacy, Meerut Institute of Technology, Meerut 250103, India

Neeraj Kant Sharma – Department of Pharmacy, Meerut Institute of Technology, Meerut 250103, India; orcid.org/0000-0001-9165-6686

Vaishali M. Patil – Charak School of Pharmacy, Chaudhary Charan Singh University, Meerut 250001, India; orcid.org/0000-0002-5352-7872

Dinesh Puri – Department of Pharmacy, Graphic Era Hill University, Dehradun 248002, India

Monika Singh – Department of Pharmacology, ITS College of Pharmacy, Ghaziabad 201206, India

Complete contact information is available at:

<https://pubs.acs.org/10.1021/acsomega.4c03774>

Notes

The authors declare no competing financial interest.

ACKNOWLEDGMENTS

This study was supported via funding from Prince Sattam bin Abdulaziz University; project number PSAU/2024/R/1445.

REFERENCES

- (1) Martínez-Iglesias, O.; Naidoo, V.; Carrera, I.; Corzo, L.; Cacabelos, R. Natural Bioactive Products as Epigenetic Modulators for Treating Neurodegenerative Disorders. *Pharmaceuticals* **2023**, *16* (2), 216.
- (2) Cho, Y. B.; Lee, H.; Jeon, H. J.; Lee, J. Y.; Kim, H. J. Antioxidant and Inhibitory Activities of *Filipendula glaberrima* Leaf Constituents Against HMG-CoA Reductase and Macrophage Foam Cell Formation. *Molecules* **2024**, *29* (2), 354.
- (3) Comini, L. R.; Montoya, S. C.; Páez, P. L.; Argüello, G. A.; Albesa, I.; Cabrera, J. L. Antibacterial Activity of Anthraquinone Derivatives from *Heterophyllaea pustulata* (Rubiaceae). *J. Photochem. Photobiol., B* **2011**, *102* (2), 108–114.
- (4) Deoda, R. S.; Kumar, D.; Bhujbal, S. S. Gastroprotective Effect of *Rubia cordifolia* Linn. on Aspirin Plus Pylorus-Ligated Ulcer. *Evid. Based Complement. Alternat. Med.* **2011**, *2011*, No. 541624.
- (5) Patil, R. A.; Jagdale, S. C.; Kasture, S. B. Antihyperglycemic, Antistress and Nootropic Activity of Roots of *Rubia cordifolia* Linn. *Indian J. Exp. Biol.* **2006**, *44* (12), 987–992.
- (6) Rani, S.; Mandave, P.; Khadke, S.; Jagtap, S.; Patil, S.; Kuvalekar, A. Antiglycation, Antioxidant and Antidiabetic Activity of Traditional Medicinal Plant: *Rubia cordifolia* Linn. for Management of Hyperglycemia. *Int. J. Plant Anim Environ. Sci.* **2013**, *14*, 42–49.
- (7) Baskar, R.; Bhakshu, L. M.; Vijaya Bharathi, G.; Sreenivasa Reddy, S.; Karuna, R.; Kesava Reddy, G.; Kumari, S. D. Antihyperglycemic Activity of Aqueous Root Extract of *Rubia cordifolia*. in streptozotocin-induced diabetic Rats. *Pharm. Biol.* **2006**, *44*, 475–479.
- (8) Joharapurkar, A. A.; Zambad, S. P.; Wanjar, M. M.; Umathe, S. N. *In-vivo* Evaluation of Antioxidant Activity of Alcoholic Extract of *Rubia cordifolia* Linn. and Its Influence on Ethanol-Induced Immunosuppressant. *Indian J. Pharmacol.* **2003**, *35*, 232–236.
- (9) Rahman, H. S.; Othman, H. H.; Hammadi, N. I.; Yeap, S. K.; Amin, K. M.; Abdul Samad, N.; Alitheen, N. B. Novel Drug Delivery Systems for Loading of Natural Plant Extracts and Their Biomedical Applications. *Int. J. Nanomedicine* **2020**, *15*, 2439–2483.
- (10) Gupta, R. K.; et al. Anti-hepatotoxic Potential of *Rubia cordifolia* Against D-Galactosamine Hepatopathy in Experimental Rodents. *Asian Pac. J. Trop. Biomed.* **2012**, *2*, 1542–1547.
- (11) Jiang, W.; Kuang, L.; Hou, A.; Qian, M.; Li, J. Iridoid Glycosides from *Hedyotis corymbosa*. *Helvetica Chimica Acta* **2007**, *90*, 1296.
- (12) Yogita, R.; Shital, S.; Aishwarya, P.; Manojkumar, N.; Shrinivas, M. Phytosomes—A Novel Approach in Herbal Drug Delivery System. *Asian J. Res. Pharm. Sci.* **2018**, *8* (3), 151–154.
- (13) Shakeel, F.; Alam, P.; Anwer, M. K.; Alanazi, S. A.; Alsarra, I. A.; Alqarni, M. H. Wound healing evaluation of self-nanoemulsifying drug delivery system containing *Piper cubeba* essential oil. *3 Biotech* **2019**, *9*, 82.
- (14) Kidd, P. M. Bioavailability and Activity of Phytosome Complexes from Botanical Polyphenols: The Silymarin, Curcumin, Green Tea, and Grape Seed Extracts. *Altern. Med. Rev.* **2009**, *14* (3), 226–246.
- (15) Vora, A.; Londhe, V.; Pandita, N. Herbosomes Enhance the *In-vivo* Antioxidant Activity and Bioavailability of Punicalagins from Standardized Pomegranate Extract. *J. Funct. Foods* **2015**, *12*, 540–548.
- (16) Sharma, S.; Sahu, A. N. Development, Characterization, and Evaluation of Hepatoprotective Effect of *Abutilon indicum* and *Piper longum* Phytosomes. *Pharmacogn. Res.* **2016**, *8* (1), 29–36.
- (17) Kaur, J.; Anwer, M. K.; Sartaj, A.; Panda, B. P.; Ali, A.; Zafar, A.; Kumar, V.; Gilani, S. J.; Kala, C.; Taleuzzaman, M. ZnO Nanoparticles of *Rubia cordifolia* Extract Formulation Developed and Optimized with QbD Application, Considering Ex Vivo Skin Permeation, Antimicrobial and Antioxidant Properties. *Molecules* **2022**, *27*, 1450.
- (18) Masduqi, A. F.; Izzati, M.; Prihastanti, E. Effect of Drying Method on Chemical Content in Sargassum Polycystum Seaweed. *Bul. Anatomi Fisiologi* **2014**, *22*, 1–9.

- (19) Ogawa, M.; Uchino, R.; Kawai, A.; Kosugi, M.; Magata, Y. PEG Modification of (111) In-Labeled Phosphatidylserine Liposomes for Imaging of Atherosclerotic Plaques. *Nucl. Med. Biol.* **2015**, *42* (3), 299–304.
- (20) Gelperina, S.; Kisich, K.; Iseman, M. D.; Heifets, L. The Potential Advantages of Nanoparticle Drug Delivery Systems in the Chemotherapy of Tuberculosis. *Am. J. Respir. Crit. Care Med.* **2005**, *172* (12), 1487–1490.
- (21) Villa-Vélez, H. A.; Telis-Romero, J.; Javier, T.; Higuera, D. M. C.; Diana, M. Effect of Maltodextrin on the Freezing Point and Thermal Conductivity of Uvaia Pulp (*Eugenia piriiformis* Cambess). *Cienc. Agrotecnol.* **2012**, *36*, 1–6.
- (22) Liu, W.; Pan, H.; Zhang, C.; Zhao, L.; Zhao, R.; Zhu, Y.; Pan, W. Developments in Methods for Measuring the Intestinal Absorption of Nanoparticle-Bound Drugs. *Int. J. Mol. Sci.* **2016**, *17* (7), 1171.
- (23) Goel, R.; Tyagi, N. Potential Contribution of Antioxidant Mechanism in the Defensive Effect of Lycopene Against Partial Sciatic Nerve Ligation Induced Behavioral, Biochemical and Histopathological Modification in Wistar Rats. *Drug Res.* **2016**, *66* (12), 633–638.
- (24) Khan, J.; Alexander, A.; Ajazuddin; Saraf, S.; Saraf, S. Recent Advances and Future Prospects of Phyto Phospholipid Complexation Technique for Improving Pharmacokinetic Profile of Plant Actives. *J. Controlled Release* **2013**, *168* (1), 50–60.
- (25) Tan, Q.; Liu, S.; Chen, X.; Wu, M.; Wang, H.; Yin, H.; He, D.; Xiong, H.; Zhang, J. Design and Evaluation of a Novel Evodiamine-Phospholipid Complex for Improved Oral Bioavailability. *AAPS PharmSciTech* **2012**, *13* (2), 534–547.
- (26) Subtil, S. F.; Rocha-Selmi, G. A.; Thomazini, M.; Trindade, M. A.; Netto, F. M.; Favaro-Trindade, C. S. Effect of Spray Drying on the Sensory and Physical Properties of Hydrolyzed Casein Using Gum Arabic as the Carrier. *J. Food Sci. Technol.* **2014**, *51* (9), 2014–2021.
- (27) Vallejo-Castillo, V.; Rodríguez-Stouvenel, A.; Martínez, R.; Bernal, C. Development of Alginate-Pectin Microcapsules by the Extrusion for Encapsulation and Controlled Release of Polyphenols from Papaya (*Carica papaya* L.). *J. Food Biochem.* **2020**, *44* (9), No. e13331.
- (28) Carabin, I. G.; Burdock, G. A.; Chatzidakis, C. Safety Assessment of *Panax Ginseng*. *Int. J. Toxicol.* **2000**, *19* (4), 293–301.
- (29) Guida, F.; De Gregorio, D.; Palazzo, E.; Ricciardi, F.; Boccella, S.; Belardo, C.; Iannotta, M.; Infantino, R.; Formato, F.; Marabese, I.; Luongo, L.; de Novellis, V.; Maione, S. Behavioral, Biochemical and Electrophysiological Changes in Spared Nerve Injury Model of Neuropathic Pain. *Int. J. Mol. Sci.* **2020**, *21* (9), 3396.
- (30) Rishal, I.; Rozenbaum, M.; Fainzilber, M. Axoplasm Isolation from the Rat Sciatic Nerve. *J. Vis. Exp.* **2010**, No. 43, 2087.
- (31) Ohkawa, H.; Ohishi, N.; Yagi, K. Assay for Lipid Peroxides in Animal Tissues by Thiobarbituric Acid Reaction. *Anal. Biochem.* **1979**, *95* (2), 351–358.
- (32) Kukkar, A.; Bali, A.; Singh, N.; Jaggi, A. S. Implications and Mechanism of Action of Gabapentin in Neuropathic Pain. *Arch. Pharm. Res.* **2013**, *36* (3), 237–251.
- (33) Prior, R. L.; Wu, X.; Schaich, K. Standardized Methods for the Determination of Antioxidant Capacity and Phenolics in Foods and Dietary Supplements. *J. Agric. Food Chem.* **2005**, *53* (10), 4290–4302.
- (34) Al Bashera, M.; Mosaddik, A.; El-Saber Batiha, G.; Alqarni, M.; Islam, M. A.; Zouganelis, G. D.; Alexiou, A.; Zahan, R. *In-vivo* and *In-vitro* Evaluation of Preventive Activity of Inflammation and Free Radical Scavenging Potential of Plant Extracts from *Oldenlandia corymbosa* L. *Appl. Sci.* **2021**, *11* (19), 9073.
- (35) Ramasarma, T.; Rao, A. V.; Devi, M. M.; Omkumar, R. V.; Bhagyashree, K. S.; Bhat, S. V. New Insights of Superoxide Dismutase Inhibition of Pyrogallol Autoxidation. *Mol. Cell. Biochem.* **2015**, *400* (1–2), 277–285.
- (36) Ellman, G. L. Tissue Sulfhydryl Groups. *Arch. Biochem. Biophys.* **1959**, *82* (1), 70–77.
- (37) Hadwan, M. H. Simple Spectrophotometric Assay for Measuring Catalase Activity in Biological Tissues. *BMC Biochem.* **2018**, *19* (1), 7.
- (38) Kanyadhara, S.; Dodoala, S.; Sampathi, S.; Punuru, P.; Chinta, G. Ethanolic Extract of Aloe vera Ameliorates Sciatic Nerve Ligation Induced Neuropathic Pain. *Anc. Sci. Life* **2014**, *33* (4), 208–215.
- (39) Solnier, J.; Zhang, Y.; Roh, K.; Kuo, Y. C.; Du, M.; Wood, S.; Hardy, M.; Gahler, R. J.; Chang, C. A Pharmacokinetic Study of Different Quercetin Formulations in Healthy Participants: A Diet-Controlled, Crossover, Single- and Multiple-Dose Pilot Study. *Evid. Based Complement. Alternat. Med.* **2023**, *2023*, No. 9727539.
- (40) Chen, W.; Balan, P.; Popovich, D. G. Analysis of Ginsenoside Content (*Panax Ginseng*) from Different Regions. *Molecules* **2019**, *24* (19), 3491.